Kinetic Studies on State-State Coupling and Collisional Quenching of Excited Sulfur Dioxide

QUN ZHANG, CONGXIANG CHEN, SHUQIN YU, XINGXIAO MA

Department of Chemical Physics, University of Science and Technology of China, Hefei, Anhui, 230026, People's Republic of China

Received 19 May 1997; accepted 20 January 1998

ABSTRACT: The time-resolved total emission of SO_2 ($B^1B_1 \rightarrow X^1A_1$) at 354.9 nm were monitored following the direct excitation by a 266 nm laser pulse. A three-level model was proposed to deal with SO_2 (X^1A_1, A^1A_2, B^1B_1) system. From a kinetic treatment of these measurements, the coupling coefficient, ξ, and the relaxation time, τ, relating to the high vibronic levels of A^1A_2 and B^1B_1 states were first obtained. It is found that ξ and τ values keep basically constant, reflecting the characteristics of the studied system. In addition, the quenching rate constants of SO_2 (A^1A_2, B^1B_1) by some alkane and chloromethane molecules were measured at room temperature. The formation cross sections of complexes of SO_2 (A^1A_2, B^1B_1) and quenchers were calculated by means of a collision complex model. It is shown that the dependence of the formation cross section of complex on the number of C—H or C—Cl bonds is generally in agreement with that of the measured quenching cross section. © 1998 John Wiley & Sons, Inc. Int J Chem Kinet 30: 831–837, 1998

INTRODUCTION

In view of the effects of sulfur dioxide pollution in the atmosphere, much effort has gone into the study of the photochemistry and photophysics of SO_2. The intrinsic complexity of the electronically excited states in the 240–340 nm region [1–4] has made the kinetic studies of single electronic state of SO_2 very difficult in this region, where several kinds of couplings happened among X^1A_1, A^1A_2, B^1B_1 states of SO_2 [5–7].

The main absorption in the near ultraviolet, 240–340 nm, has been assigned to transitions into the A^1A_2 state which borrows intensity through vibronic coupling with the neighboring B^1B_1 state [5,6]. The latter is intensively perturbed through Renner–Teller coupling with the ground state [7] and excitation into the B^1B_1 state is associated with a weak underlying "quasi-continuum" in the absorption spectrum. The studies of single vibronic level fluorescence spectra by Shaw et al. [8,9] gave credence to the explanation that the bulk of the emission is due to the B^1B_1 levels spread among the A^1A_2 levels.

Most of the previous kinetic studies on SO_2 in the 240–340 nm region have been dealing with A^1A_2 and B^1B_1 separately and have much controversy [1]. Here, we propose a three-level model to process SO_2 (X^1A_1, A^1A_2, B^1B_1) system. According to this model, the kinetic behavior of A^1A_2 and B^1B_1 is regarded as unity.

Correspondence to: C. Chen

Contract grant Sponsor: National Natural Science Foundation Committee of China

Contract grant Sponsor: University of Science and Technology of China

Contract grant Sponsor: Tokyo University

 CCC 0538-8066/98/110831-07

EXPERIMENTAL METHOD

The experiments were performed in a stainless steel reactor. The experimental arrangement was described in detail previously [10]. SO_2 molecule and the quenching molecules were diluted in the bath gas, He, and stored in 10 l reservoirs prior to experiments. Three gas mixtures flowed continuously into the reaction vessel: f_1, a flow of about 6.6% SO_2 in He; f_2, a flow of the quenching molecule mixed with He; and f_3, a flow of pure He. Keeping f_1 and the sum of f_2 and f_3 constant, the ratio of f_2 to f_3 was varied, resulting in a change of the concentration of added quenchers in the reaction vessel. The three flows were measured by massflowmeters. The total pressure was about 5 torr and the partial pressure of SO_2 in the reaction vessel was about 150 m torr. The quadrupled YAG laser at 266 nm was focused by a lens with focal length of 50 cm and irradiated into the center of the reactor. SO_2 (A^1A_2, B^1B_1) was populated by absorption of radiation from a 266 nm laser pulse. The spontaneous fluorescence of SO_2 ($B^1B_1 \rightarrow X^1A_1$) was collected by a lens with 5 cm focal length and focused into the entrance slit of a monochromator. A photomultiplier was connected onto the exit slit of the monochromator. The photomultiplier output was taken to a digital storage oscilloscope. A microcomputer was interfaced with a digital oscilloscope allowing software control of the data collection and signal averaging. Before analysis of the time-resolved signal, a small background signal, which is resulted from the laser irradiation of the empty reactor, was subtracted from the gross signal to get a net value. The digital oscilloscope was triggered by the output of a photodiode which was irradiated by the doubled YAG laser at 532 nm.

He (99.999%, Wuxi) was used without further purification. Added gases *n*-C_5H_{12}, *n*-C_6H_{14}, *n*-C_7H_{16}, CH_2Cl_2, $CHCl_3$, and CCl_4 were all analytical reagent grade. CH_3Cl (C.P. grade) and SO_2 (anhydrous grade) were purified further by freeze-pump-thaw cycles in a vacuum.

DESCRIPTION OF KINETIC MODEL

The kinetic processes of SO_2 (X^1A_1, A^1A_2, B^1B_1) system which is produced by 266 nm laser excitation are

$$X \xrightarrow{266\text{nm}} A \quad \text{and} \quad B \qquad \text{main absorption} \qquad \text{(a)}$$

$$A \xrightarrow{\xi_1} B \qquad \text{(b)}$$

$$B \xrightarrow{\xi_2} A \qquad \text{(b)}$$

$$A(B) + M \xrightarrow{k_M^A(k_M^B)} X + M \quad \text{or other products} \qquad \text{(c)}$$

$$A(B) + Q \xrightarrow{k_Q^A(k_Q^B)} X + Q \quad \text{or other products} \qquad \text{(d)}$$

$$A \xrightarrow{k_f^A} X + h\nu_f{}^A \qquad \text{(e)}$$

$$B \xrightarrow{k_f^B} X + h\nu_f{}^B \qquad \text{(e)}$$

where X, A, and B represent X^1A_1, A^1A_2, and B^1B_1 states, respectively. Q is quencher, M is other molecules (including SO_2, He, etc.) than Q.

In order to deal with more detailed information about SO_2 (X^1A_1, A^1A_2, B^1B_1) system, we think it is necessary to investigate a general three-level model which is schematically shown in Figure 1. Since what we shall discuss afterwards is a fast-pump process (the pulse width of YAG laser is 8 ns) and laser intensity is not too high (5–10 mJ/pulse, focal length is 50 cm), we assume pump and dump will not influence the description of kinetic behavior after laser irradiation [11].

Immediately after laser pulse, we assume the partial densities of level 1 and 2 are N_{10} and N_{20}, respectively. In Figure 1, A_i, q_i, and ξ_i ($i = 1, 2$) represent the Einstein spontaneous emission coefficients, the quenching rates, and the transition rates of level 1 and 2, respectively.

The kinetic equations of N_1 and N_2 can be expressed as

$$\frac{dN_1}{dt} = -(A_1 + q_1 + \xi_1)N_1 + \xi_2 N_2 \qquad (1)$$

$$\frac{dN_2}{dt} = \xi_1 N_1 - (A_2 + q_2 + \xi_2)N_2 \qquad (2)$$

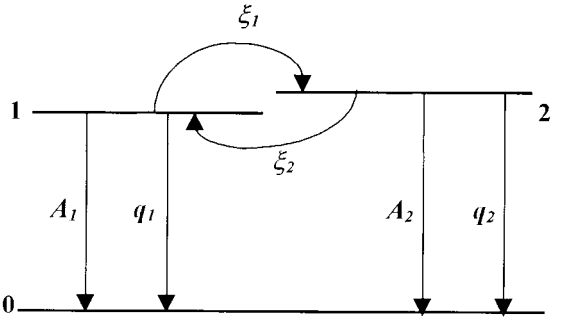

Figure 1 Schematic diagram of a three-level model.

$$(N_1, N_2)_{t=0} = (N_{10}, N_{20}) \quad (3)$$

Equations (1) and (2) can be simplified as

$$\frac{dN_1}{dt} = -AN_1 + BN_2 \quad (4)$$

$$\frac{dN_2}{dt} = CN_1 - DN_2 \quad (5)$$

where

$$A = A_1 + q_1 + \xi_1, \quad B = \xi_2, \quad C = \xi_1, \quad D = A_2 + q_2 + \xi_2 \quad (6)$$

Meanwhile we assume

$$\alpha + \beta = A + D, \quad \alpha\beta = AD - BC, \quad \beta > \alpha > 0 \quad (7)$$

Thus, we can arrive at

$$N_1 = \frac{1}{\beta - \alpha}\{[(\beta - A)N_{10} + BN_{20}]e^{-\alpha t} + [(A - \alpha)N_{10} - BN_{20}]e^{-\beta t}\} \quad (8)$$

$$N_2 = \frac{1}{\beta - \alpha}\{[CN_{10} + (A - \alpha)N_{20}]e^{-\alpha t} - [CN_{10} - (\beta - A)N_{20}]e^{-\beta t}\} \quad (9)$$

Noting ξ_1, $\xi_2 \gg (A_1 + q_1)$, $(A_2 + q_2)$, α and β can be simplified as

$$\alpha \approx \frac{\xi_2 A_1 + \xi_1 A_2}{\xi_1 + \xi_2} + \frac{\xi_2 k_{q1} + \xi_1 k_{q2}}{\xi_1 + \xi_2}[Q] \quad (10)$$

$$\beta \approx \xi_1 + \xi_2 \quad (11)$$

where

$$k_{q1}[Q] = q_1, \quad k_{q2}[Q] = q_2 \quad (12)$$

k_{q1} and k_{q2} are second-order quenching rate constants of level 1 and 2, respectively. [Q] is the concentration of quenching molecule.

Consequently equations (8) and (9) can be simplified as

$$N_1 = \frac{1}{\xi_1 + \xi_2}[\xi_2(N_{10} + N_{20})e^{-\alpha t} + (\xi_1 N_{10} - \xi_2 N_{20})e^{-\beta t}] \quad (13)$$

$$N_2 = \frac{1}{\xi_1 + \xi_2}[\xi_1(N_{10} + N_{20})e^{-\alpha t} - (\xi_1 N_{10} - \xi_2 N_{20})e^{-\beta t}] \quad (14)$$

When $\xi_1 N_{10} > \xi_2 N_{20}$, N_1 is a sum of two exponential decay terms, while one exponential decay term subtracted from another gives N_2. Equations (13) and (14) reflect kinetic behavior of "donor state" (N_1) and "acceptor state" (N_2), respectively.

Let $\xi = \beta$, i.e.,

$$\xi = \xi_1 + \xi_2 \quad (15)$$

Here, ξ is called coupling coefficient between level 1 and 2.

The time-resolved fluorescence signals of excited SO_2 at 354.9 nm can all be divided into ascending part and descending one. From the semilogarithmic plot of a typical signal (Fig. 2), we can see that the descending part is a broken line, which tells us the fluorescence signals should be determined by eq. (14), i.e., the fluorescence emission of excited SO_2 is supposed to be from "acceptor state". In SO_2 (X^1A_1, A^1A_2, B^1B_1) system, the "acceptor state" is thought to be B^1B_1 state [8,9].

According to the above-mentioned three-level model, we can arrive at

$$[B] = \frac{1}{\xi}[\xi_1([A]_0 + [B]_0)e^{-Kt} - (\xi_1[A]_0 - \xi_2[B]_0)e^{-\xi t}] \quad (16)$$

where

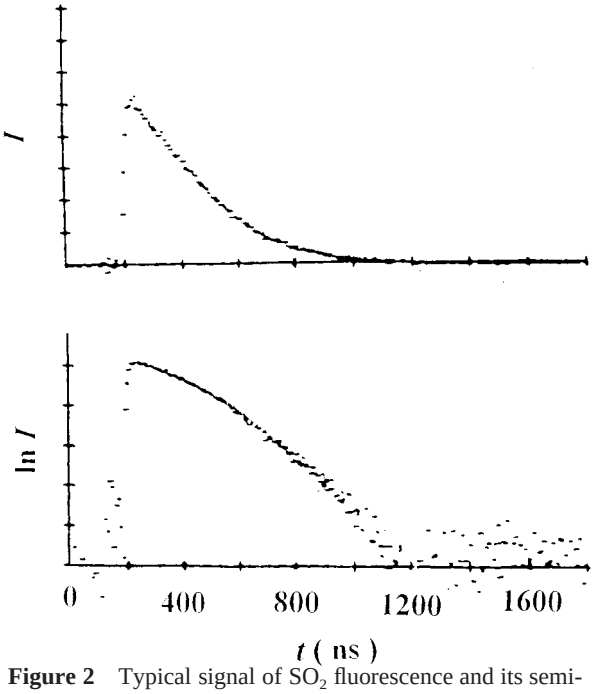

Figure 2 Typical signal of SO_2 fluorescence and its semilogarithmic plot.

$$K = k_f + \sum_{\mathrm{M}} k_{\mathrm{M}}[\mathrm{M}] + k_{\mathrm{Q}}[\mathrm{Q}] \quad (17)$$

$$k_f = \frac{\xi_2 k_f^{\mathrm{A}} + \xi_1 k_f^{\mathrm{B}}}{\xi} \quad (18)$$

$$k_{\mathrm{M}} = \frac{\xi_2 k_M^{\mathrm{A}} + \xi_1 k_M^{\mathrm{B}}}{\xi} \quad (19)$$

$$k_{\mathrm{Q}} = \frac{\xi_2 k_Q^{\mathrm{A}} + \xi_1 k_Q^{\mathrm{B}}}{\xi} \quad (20)$$

Formula (20) shows that the quenching of SO_2 excited by 266 nm laser pulse includes the quenching of both A^1A_2 and B^1B_1 states by coupling of these two states.

Since the fluorescence intensity is proportional to [B], the detected signal I should appear with the same double exponential decay behavior as [B], i.e.,

$$\mathrm{I} = f k_f^{\mathrm{B}} [\mathrm{B}] = \mathrm{I}_1 \exp(-Kt) - \mathrm{I}_2 \exp(-\xi t) \quad (21)$$

Utilizing PLOT-50 software to fit the detected signal I, we can obtain ξ and K. Here, let $\tau = \frac{1}{\xi}$, τ is called the relaxation time of the coupling equilibrium between A^1A_2 and B^1B_1. Considering that the total pressure in the reaction vessel and SO_2 partial pressure are constant in our experiment, and the concentration of quenching molecules is far higher than that of excited SO_2 molecules, formula (17) can be simplified as

$$K = k_q[q] + \text{Const.} \quad (22)$$

The second-order quenching rate constant k_q is the slope of the linear plot of the first-order decay rate constant K vs. the concentration of added quencher, namely [Q].

In addition, we can get the quenching cross section σ_q according to the following equation

$$\sigma_q = k_q/\mathrm{V} \quad (23)$$

where $\mathrm{V}(=[8kT/(\pi\mu)]^{1/2})$ is the averaged relative kinetic velocity.

RESULTS AND DISCUSSION

ξ and τ

The coupling coefficient ξ and the relaxation time τ under different experimental conditions are summarized in Table I–III. From these values, it is found that the order of magnitude of ξ is $10^7\ s^{-1}$ and τ varies slightly from about 30 ns to 80 ns. We can draw a conclusion that ξ and τ have little to do with collision, at least under our experimental conditions. Since $\xi = \xi_1 + \xi_2$ and $\tau = 1/\xi$, ξ and τ should only be determined by the transition rates of excited SO_2 in its high vibronic levels belonging to A^1A_2 and B^1B_1 states. So it is assumed ξ and τ are not to be influenced by the concentration of added quenchers, the quality of collision partners and the total pressure of the experimental system. We can reach a conclusion that the constancy of ξ and τ values reflects the intrinsic characteristics of SO_2 (X^1A_1, A^1A_2, B^1B_1) system.

Table I ξ and τ Values for the Same Collision Partner at Different Concentration of CH_2Cl_2 (λ = 354.9nm)

$[CH_2Cl_2]$ (10^{15} molecule cm^{-3})	ξ ($10^7\ s^{-1}$)	τ (ns)
0	1.48 ± 0.08	68 ± 4
2.59	1.41 ± 0.08	71 ± 4
5.38	1.28 ± 0.08	78 ± 5
8.07	1.84 ± 0.12	54 ± 4
10.76	1.89 ± 0.13	53 ± 4
13.21	1.95 ± 0.14	51 ± 4
16.15	1.46 ± 0.09	68 ± 4
20.18	1.35 ± 0.09	74 ± 5
Average value	1.58 ± 0.27	65 ± 10

k_q and σ_q

For example, the time-resolved fluorescence signal of SO_2 ($B \rightarrow X$) and its semilogarithmic plot with $CHCl_3$ being quencher are shown in Figure 2 (see section 3). The Stern–Volmer plot of first-order decay rate constant K vs. $[CHCl_3]$ is shown in Figure 3. The measured quenching rate constants and corresponding cross sections of SO_2 (A, B) by some alkane and chloromethane molecules are given in Table IV.

Following a method based on a collisional complex model [12,13], we calculated the complex formation

Table II ξ and τ Values for Different Collision Partners (λ = 354.9nm)

Quencher	T(K)	$\xi(10^7\ s^{-1})$	τ(ns)
He	289	1.66 ± 0.14	61 ± 6
CH_3Cl	291	3.01 ± 0.46	34 ± 7
CH_2Cl_2	295	1.58 ± 0.27	65 ± 10
$CHCl_3$	293	3.00 ± 0.56	34 ± 5
CCl_4	291	2.55 ± 0.19	39 ± 3
n-C_5H_{12}	291	2.34 ± 0.64	46 ± 14
n-C_6H_{14}	291	3.03 ± 0.65	34 ± 7
n-C_7H_{16}	290	1.42 ± 0.24	72 ± 13
Average value		2.36 ± 0.65	47 ± 15

Table III ξ and τ Values for Different Pressure of Pure SO_2 Gas (λ = 354.9nm)

P_{SO_2} (torr)	$\xi(10^7\ s^{-1})$	τ(ns)
0.16	3.41 ± 0.18	29 ± 1
0.40	3.75 ± 0.23	27 ± 2
0.64	2.53 ± 0.14	40 ± 2
1.76	2.91 ± 0.29	34 ± 3
2.16	3.49 ± 0.43	29 ± 4
7.92	3.77 ± 0.27	27 ± 2
Average value	3.31 ± 0.49	31 ± 5

Table IV Quenching Rate Constants k_q and Cross Sections σ_q for $SO_2(A^1A_2, B^1B_1)$ at 290 ± 5 K

Quencher	T(K)	$k_q(cm^2\ molec^{-1}\ s^{-1})$	$\sigma_q(10^{-2}\ nm^2)$
He	289	2.08 ± 0.12	1.17 ± 0.07
CH_3Cl	291	9.22 ± 0.49	19.7 ± 1.1
CH_2Cl_2	295	10.6 ± 1.0	25.6 ± 2.3
$CHCl_3$	293	12.1 ± 1.0	31.4 ± 2.6
CCl_4	291	15.3 ± 0.6	41.5 ± 1.6
n-C_5H_{12}	291	10.4 ± 0.5	24.3 ± 1.3
n-C_6H_{14}	291	13.7 ± 0.7	33.3 ± 1.7
n-C_7H_{16}	290	20.3 ± 0.4	51.2 ± 1.0

cross section σ_{cf} of SO_2 (A^1A_2 and B^1B_1) with the above-mentioned quenchers. The parameters used in the calculation, the experimentally measured quenching cross sections, and calculated complex formation cross sections are summarized in Table V.

The quenching of SO_2 (A, B) is a complicated process, including not only physical quenching but also chemical one. From Table IV, it is shown that k_q bears 10^{-10} cm^3 $molec^{-1}$ s^{-1} in order of magnitude. Generally, such order of magnitude indicates the quenching process is mainly due to the contribution of chemical reaction [19].

From Table IV, we can also see that the quenching rate constants and cross sections all increase with increasing the number of C—H or C—Cl bonds. It is shown in Table V that the dependence of the formation cross section of complex on the number of C—H bonds contained in alkane molecules is in agreement with that of the measured quenching cross section. This tendency might be accountable to the increase of dipole and quadruple moments, polarization ratio, and dispersion force with increasing the number of C—H bonds. As for chloromathane molecules, however, σ_{cf} increases from CH_3Cl to CH_2Cl_2, then decreases from CH_2Cl_2 to CCl_4, which obviously deviates from

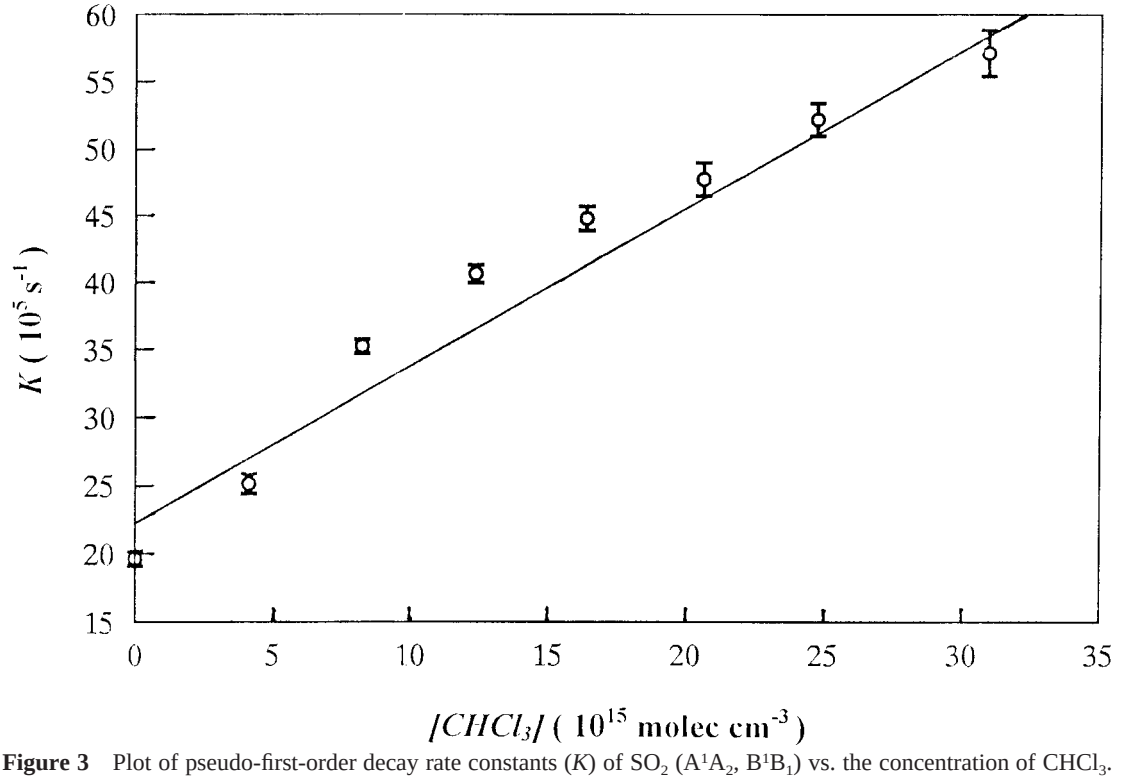

Figure 3 Plot of pseudo-first-order decay rate constants (K) of SO_2 (A^1A_2, B^1B_1) vs. the concentration of $CHCl_3$.

Table V Calculated Complex Formation Cross Sections σ_{cf} and Measured Quenching Cross Sections σ_q at Room Temperature with Parameters Used in Calculation

Quencher	μ[a] (D)	α[a] (10^{-3}nm^3)	Q[c] (10^{-26}esu•cm^2)	I.P.[a] (eV)	σ_q(10^{-2}nm^2) SO_2(A,B)	σ_{cf}(10^{-2}nm^2) Max. SO_2(A) SO_2(B)	σ_{cf}(10^{-2}nm^2) Ave. SO_2(A) SO_2(B)
SO_2(A)	1.63[b]	3.89[b]	4.40	8.87			
SO_2(B)	1.59	3.72	4.40	8.37			
He	0.00	0.21	0.00	24.6	1.17 ± 0.07	31.31	30.89
						30.44	30.02
CH_4	0.00	2.59	0.00[d]	12.6		68.15	67.01
						66.44	65.30
C_2H_6	0.00	4.47	0.65[d]	11.5		84.18	79.63
						82.19	77.66
C_3H_8	0.08	6.37	1.50[e]	11.1		100.9	89.82
						98.70	87.66
n-C_4H_{10}	0.03	8.20	2.00[e]	10.6		107.4	97.32
						105.0	95.02
n-C_5H_{12}	0.10	9.99	2.60	10.4	24.3 ± 1.3	118.3	103.9
						115.8	101.5
n-C_6H_{14}	0.05	11.9	3.00	10.2	33.3 ± 1.7	123.3	109.9
						120.6	107.4
n-C_7H_{16}	0.10	13.7	3.50	9.90	51.2 ± 1.0	131.2	115.0
						128.4	112.3
CH_3Cl	1.87	4.72	1.23[e]	11.3	19.7 ± 1.1	164.5	95.75
						162.1	93.99
CH_2Cl_2	1.60	6.48	4.10[d]	11.4	25.6 ± 2.3	169.5	107.5
						166.9	105.4
$CHCl_3$	1.01	9.50	3.50	11.4	31.4 ± 2.6	154.4	107.6
						151.7	105.2
CCl_4	0.00	11.2	0.00[d]	11.5	41.5 ± 1.6	109.7	107.8
						107.0	105.1

[a] Ref. [14].
[b] Ref. [15].
[c] Ref. [16].
[d] Ref. [17].
[e] Ref. [18].

the progressively increasing tendency of σ_q. This deviation may result from the ignorance of activation barrier in calculation. In addition, the σ_{cf} of SO_2 (A) is larger than the corresponding value of SO_2 (B), because the dipole moment and polarization ratio of SO_2 (A) may be larger than that of SO_2 (B). From the above discussion, a general conclusion can be drawn that multiple attractive forces play an important role in the quenching of electronically excited SO_2 (A^1A_2, B^1B_1) molecules.

We appreciate financial support by the National Natural Science Foundation Committee of China and the cooperation research project between University of Science and Technology of China and Tokyo University.

BIBLIOGRAPHY

1. J. Heiklen, N. Kelly, and K. Partymiller, *Rev. Chem. Intermediates*, **3,** 315 (1980).
2. E. Hegazi, A. Hamdan, and F. Al-Adel, *Chem. Phys. Lett.*, **221,** 33 (1994).
3. S. L. Manatt, and A. L. Lane, *J. Quant. Spectrosc. Rad. Transfer*, **50,** 267 (1993).
4. V. Prahlad, S. M. Ahmed, and V. Kumar, *J. Quant. Spectrosc. Rad. Transfer*, **56,** 57 (1996).
5. Y. Hamada, and A. J. Merer, *Can. J. Phys.*, **52,** 1443 (1974).

6. Y. Hamada, and A. J. Merer, *Can. J. Phys.*, **53,** 2555 (1975).
7. P. J. Gardner, *Chem. Phys. Lett.*, **4,** 167 (1969).
8. R. J. Shaw, J. R. Kent, and M. P., O'Dwyer, *J. Mol. Spectrosc.*, **82,** 1 (1980).
9. R. J. Shaw, J. R. Kent, and M. P. O'Dwyer, *Chem. Phys.*, **18,** 151, 165 (1976).
10. C. X. Chen, X. J. Wang, S. Q. Yu, and X. X. Ma, *Chem. Phys. Lett.*, **197,** 286 (1992).
11. X. X. Ma and F. A. Kong, *Laser Chemistry*, USTC Press, Hefei, 1990, p. 30.
12. P. W. Fairchild, G. P. Smith, and D. R. Crosley, *J. Chem. Phys.*, **79,** 1795 (1983).
13. J. O. Hirschfelder, C. F. Curtis, and R. B. Bird, *Molecular Theory of Gases and Liquids*, ed. by Wiley (London, 1954), 26.
14. D. R. Lide, *CRC Handbook of Chemistry and Physics 71st Edition*, 1990–1991 (CRC Press Inc., Florida, 1991).
15. D. L. Holtermann, and E. K. C. Lee, *J. Chem. Phys.*, **77,** 5327 (1982).
16. R. A. Copeland, M. J. Dyer, and D. R. Crosley, *J. Chem. Phys.*, **82,** 4022 (1985).
17. D. E. Stogryn, and A. P. Stogryn, *Mol. Phys.*, **11,** 371 (1966).
18. D. L. Vanderhart, and W. H. Flygare, *Mol. Phys.*, **18,** 77 (1970).
19. C. J. Nokes, and R. J. Donovan, *Chem. Phys.*, **90,** 167 (1984).